# Portable Device to Assist with Force Control in Ultrasound Acquisition

Huayang Sai, Lijuan Wang, Jie Zhang, Chengkai Xia, and Zhenbang Xu

*Abstract*—**This study presents a portable device that ensures precise contact force between a subject and a probe to improve the stability and reproducibility of ultrasound (US) acquisition. The mechanical portion of the device includes a servo motor, gears, and a ball screw linear actuator; two photoelectric switches are used to limit the stroke. A combined force and position control system is developed, and a pressure threshold is introduced to reduce the chattering of the system so that it can be applied to US examinations of tissues of different stiffness levels. Force control experiments were conducted on the device, and the results showed that the device can overcome the chattering of a physician's hand and movement caused by a subject's respiration. Additionally, the stability of the US acquisition was substantially improved. Based on clinical trials on humans, this device was observed to improve the consistency of ultrasonic results and the repeatability of images, and it assisted sonographers with maintaining suitable contact force and improving imaging quality. The device can either be handheld by a physician or easily integrated with a manipulator as an autonomous robotic US acquisition device, thereby validating its potential for US applications.**

*Index Terms*—**Force control, portable device, threshold, ultrasound diagnosis**

## I. INTRODUCTION

**A**MONG many medical detection methods, ultrasound (US) imaging has been widely used, owing to its cost effectiveness, non-invasiveness, and absence of ionizing radiation [1]. Typical applications of US imaging include fetal imaging, tumor detection [2], biopsy-needle-insertion monitoring [3], [4], and skeletal muscle imaging [5]. The broad application of US technology warrants the further improvement of its imaging quality and diagnostic ability, which have both become problems in healthcare.

Huayang Sai. Author is with the CAS Key Laboratory of On-orbit Manufacturing and Integration for Space Optics System, Changchun Institute of Optics, Fine Mechanics and Physics, Chinese Academy of Sciences, Changchun 130033, China, and he is now with the University of Chinese Academy of Sciences, Beijing 100049, China. (e-mail: saihuayang18@mails.ucas.ac.cn).

Lijuan Wang, was with Neuroscience Center, Department of Neurology, First Hospital of Jilin University, Jilin University, Changchun, China (e-mail: wanglj66@jlu.edu.cn).

Jie Zhang, was with Neuroscience Center, Department of Neurology, First Hospital of Jilin University, Jilin University, Changchun, China (e-mail: zhangj_0106@jlu.edu.cn).

Chengkai Xia. Author is with the CAS Key Laboratory of On-orbit Manufacturing and Integration for Space Optics System, Changchun Institute of Optics, Fine Mechanics and Physics, Chinese Academy of Sciences, Changchun 130033, China, and he is now with the University of Chinese Academy of Sciences, Beijing 100049, China. (e-mail: xiachengkai19@mails.ucas.ac.cn).

Zhenbang Xu. Author is with the CAS Key Laboratory of On-orbit Manufacturing and Integration for Space Optics System, Changchun Institute of Optics, Fine Mechanics and Physics, Chinese Academy of Sciences, Changchun 130033, China. (Corresponding author: e-mail: xuzhenbang@ciomp.ac.cn).

The contact force between a US probe and tissue can significantly impact US imaging quality, because human blood vessels and muscles are deformed in varying degrees under different pressures. An excessive contact force may deform the target anatomy or even injure the subject, whereas an insufficient contact force does not provide good acoustic coupling, thereby affecting the image quality [6]. The sonographers' ability to perceive force often decreases with time gradually, and they may even have involuntary hand tremors. Moreover, subjects experience inevitable organ movement and breathing, which can also affect image quality. In addition, the position, orientation, and contact force of the probe with the body surface are entirely determined by the experience of the sonographers. Therefore, it may be difficult to repeat the diagnosis even with the same sonographer. This leaves the sonographer potentially unable to determine if a tumor has grown over time or whether changes in diagnostic conditions have led to misleading changes in the images. Moreover, direct contact between sonographers and subjects increases vulnerability to infectious diseases, especially during a pandemic, such as the COVID-19 pandemic [7]. Finally, excessive workload exposes sonographers to a substantial increase in the probability of developing musculoskeletal disorders [8]–[10].

US elastography is a technique for estimating the elastic properties of tissue based on US images, benefiting from a controlled force. In many tissues, obtaining accurate modulus of elasticity of tissues is important for the assessment of the condition because the modulus of elasticity is closely related to tissue health [11], [12]. Currently, elastography methods require relying on excellent estimates of stress to obtain accurate elastograms, thus improving the reproducibility of elastography or enabling the assessment of elastic nonlinearity of tissues [13], [14]. In [15], Burcher *et al.* designed a handheld device that can measure contact force for quantitative investigations of deformation. Gendin *et al.* [16] investigated the reproducibility of nonlinear elasticity in breast cancer by means of a uniaxial compression device with force feedback. It is evident that elastography relies on the operator's perception of pressure, which has led to the development of more reliable and flexible hardware devices to assist the operator in obtaining the desired pressure more easily.

To address the above-mentioned challenges of freehand US equipment, a series of mechanical devices have been recently proposed to aid US diagnosis. These devices can be classified into two categories: 1) robotic US acquisition devices that are developed by combining equipment, such as manipulators and US probes that are typically installed directly on the manipulator, and 2) handheld auxiliary US diagnostic devices.

Robotic US acquisition devices are typically characterized by their large size, which is fixed by grounding; therefore, sonographers are not required to perform US examinations with the probe in hand. Benefiting from the rapid development of robotics, Pierrot *et al.* [17] developed the Hippocrate US robot, which was combined with an industrial six-axis manipulator with safety controls and a user-friendly graphical interface, to monitor arteries and prevent cardiovascular diseases. Huang *et al.* [18], [19] designed a robotic US system for three-dimensional (3D) imaging of the human skin; the system could hold a probe for 3D-US acquisitions in general applications. Recently, Welleweerd *et al.* [20] combined a 7-degree-of-freedom (DOF) robot with a linear US transducer to acquire two-dimensional (2D)-US images of the breast along a predefined trajectory. Jiang *et al.* [21], [22] proposed a robotic angular positioning method to ensure that the US probe remains perpendicular to the tissue surface and corrects the tissue deformation caused by the robot in US acquisition by a stiffness-based method. Suligoj *et al.* [23] used impedance technology to enable the US probe mounted at the end of the manipulator always be in contact with the tissue. All the above technologies are used to enable the application of robots for autonomous US diagnosis by investigating collaborative robot control technologies. Moreover, some robotic devices do not rely on existing robots but are developed independently, such as Zhu *et al.* [24]–[26] designed a 6-DOF linkage mechanism for ultrasonic carotid diagnosis that can generate a maximum force of 10 N on the probe. Benefiting from the precise angular adjustment of a parallel structure, Simon *et al.* [27] developed a parallel robot for US diagnosis and enhanced safety by applying a method used for static balancing. Vilchis *et al.* [28], [29] designed a parallel cable-driven robot that allows flexible remote US image acquisition of the abdomen of subjects; however, the contact force between the probe and the human body was not easily adjustable. The motion of the US probe in the above-mentioned systems is entirely user-directed; therefore, the workload remains heavy, and the imaging quality is dependent on the operators. Additionally, the large size and complex remote operation limit the practical application of such devices.

Handheld devices used to assist in US diagnosis tend to be more compact and portable than robotic US devices. Michael *et al.* [15] designed a handheld system that can simultaneously record the probe position, contact force, and US images. Furthermore, Tyler *et al.* [30] designed a small handheld US device, and the experimental results of their study showed that the system could adequately characterize the detection force and direction, as well as effectively synchronize all data. Gilbertson *et al.* [31], [32] designed an ergonomic handheld US device that measures the contact force and torque on the probe. Although all the above-mentioned devices can record contact force and be used to reproduce US images, the contact force is still entirely controlled by the sonographer's hand, and it cannot be adjusted autonomously. Implementing automatic adjustment of the probe position is a straightforward way to address the force variations caused by a sonographer or subject's motion. Eura *et al.* [33] and Marchal *et al.* [34] designed freehand devices to compensate for physiological

motion, but the large size and mass were not user-friendly for sonographers to hold. The MIT scholars have successively developed three generations of handheld force-controlled US devices that can stabilize the force applied to a subject by a sonographer to a desired contact force [35]–[39]. However, the controllers for these devices are bulky, and they require an external computer for interaction. Overly complex devices compete for the operator's attention; therefore, the devices and the control system should be streamlined and easy to implement. Moreover, these devices are only suitable for US examinations of the soft tissue of the body, and uncontrollable tremor occurs when they come into contact with rigid tissues, such as bones.

To assist sonographers in improving the quality of US examinations and obtaining a better interactive experience, this study aims to design a portable ultrasonic auxiliary device (PUAD) to achieve high accuracy and probe-contact-force stability. The novel contributions of this study are as follows:

1) The PUAD is primarily driven by a servo motor, gears, and a ball screw drive, and it achieves a linear reciprocating probe motion, which can meet the requirements of attaining a large pressure. Therefore, the movement of a sonographer's hand, and a subject's organ movement and breathing can be compensated to maintain the probe at the desired pressure.
2) By introducing the pressure threshold, the chattering of the device is alleviated; therefore, it can be applied to US examinations of tissues with different hardness levels.
3) Sonographers can perform tasks by holding the device, thereby improving the imaging quality of US images and reducing their reliance on operational experience. A series of clinical trials were conducted; the local ethics committee approved the experiments, and informed consent was obtained from participants.
4) The application potential of integrating the device into a robotic manipulator, instead of utilizing it only for freehand US examinations, was experimentally explored.

The remainder of this paper is organized as follows. In Section II, the mechanical and electronic designs of the PUAD are presented. In Section III, the control system of the device and the modeling and simulation of the system are presented. Section IV presents six experiments, including experiments that verify the performance of the device and a series of experiments conducted in the clinic. Section V discusses the experimental results and highlights the safety, limitations of the study and future research directions. The conclusions are presented in Section VI.

## II. MECHANICAL AND ELECTRICAL DESIGN

In this section, we present the mechanical structure and electrical system of the designed PUAD and analyze its potential to be integrated with robotic manipulators.

### A. Mechanical structure design

The PUAD mechanical design, shown in Fig. 1, includes a holdable shell and an internal mechanical structure. The maximum size of the designed housing is $54 \text{ mm} \times 67 \text{ mm} \times$

179 mm, and the structural size that is convenient for hand-holding is 32 mm × 43 mm × 158 mm, and the mass of the device is 910 g. Compared to the handheld devices in [33], [35], [40], both the size and weight are more portable and facilitate the sonographer's freehand operation. The designed PUAD is powered by a servo motor (ECXTQ22L, Maxon Group, Switzerland) with an encoder (ENX 22, Maxon Group, Switzerland) at the end of the motor to ensure accurate and reproducible position measurements. A spur gear transmits the power from the servo motor to a ball screw, thereby transforming the rotary motion into the linear motion of a slider, which drives the reciprocating linear motion of the probe. A miniature pressure sensor (LSB201, Futek, USA) is mounted at the end of the slider, and the contact force between the US probe and a subject is fed back to the control system. The probe is clamped on an adjustable clamping mechanism that clamps probes of different shapes and sizes for US examinations of different parts of the body. To prevent the actuator of the device from reaching the travel limit, two photoelectric sensors are fixed to the travel limit of the slider, enabling a maximum travel of 55 mm.

For portability, the designed PUAD can be placed in a control box with a size of 305 mm × 425 mm × 165 mm, and the total mass of the control box is about 6.8 kg. The exterior of the box comprises a power switch, data storage interface, and programmable logic controller (PLC) screen for human-machine interaction. Inside the control box, the power supply, PLC, signal amplifier, and motor controller are reasonably arranged, and a cooling fan is used to dissipate heat from the box to avoid the excessive temperature inside the control box. Additionally, sufficient space is reserved in the control box for accessories, such as the handle for sonographers to hold and accessories for the connection between the PUAD and manipulator. A cushioning sponge is arranged inside the control box to ensure that the controller is not damaged during transportation. Different from the robotic US devices in [17]–[20], the designed PUAD, as well as the controller, interactive screen, and actuator are integrated into a box that is easy to take with the sonographer. Moreover, compared to the devices mentioned in [31], [37], the designed device does not require any external device, such as a computer screen, and the device can be operated only through the interactive screen, which makes the device much more portable.

### B. Electronic and software design

The central controller of the PUAD is the PLC (SC200SMART, Siemens, Germany), owing to its cost-effectiveness and expandable touch screen. A pressure sensor transmits signal to the PLC through an amplifier and compares it with the desired pressure value set by the operator. The pressure error is then used as an input signal to pass the control command to the motor drive via the designed proportional-derivative (PD) controller on the PLC. If the probe position exceeds the stroke limit, the photoelectric sensor sends a signal to the PLC to stop the motor. Meanwhile, the PUAD is able to achieve fast start-up to ensure that it is always available.

The human–machine interface is developed using WinCC (Siemens, Germany). With the force control mode, the sono-grapher can set the desired pressure and threshold via the touch screen, as well as collect data and reset the probe position. Position control mode allows the sonographer to arbitrarily adjust the position of the probe. Meanwhile, the touch screen displays the real-time position of the US probe and the contact-force-variation curve. Therefore, the designed device can be operated after a simple introduction, without the heavy learning cost of operating a robotic manipulator.

### C. Integration of PUAD with manipulators

US scanning of patients using manipulators mitigates the risks associated with direct contact between a sonographer and a subject. However, operating a manipulator to perform US examinations on subjects is difficult for sonographers, and the installation of torque sensors on the robotic joints is expensive.

For freehand US examinations, sonographers must hold the US probe, slide it along the skin, press it into the body, and apply pressure to produce a good diagnostic image. As shown in Fig. 2, the PUAD can be mounted at the end of the manipulators as a robotic US system to perform examinations instead of freehand US system. The robotic US system can provide the flexibility to perform various forms of US scanning through the rotation of each joint of the robotic manipulator and the linear motion of the PUAD. The robotic manipulator can achieve precise position movement, and the PUAD automatically maintains the desired contact force of the probe, thereby reducing the operational difficulty of controlling the position and force simultaneously. Moreover, the PUAD has good adaptability to different manipulators, and it is easy to install at the end of different manipulators using a connector.

## III. CONTROL SYSTEM DESIGN

This section briefly describes the control strategy of the PUAD system, including the design of the pressure threshold and the combined force and position control system.

### A. Setting of the pressure threshold

The contact force between the probe and subject can be expressed by the following impedance relationship [41]:

$$K_d x + B_d \dot{x} = F_c, \qquad (1)$$

where $K_d$ and $B_d$ are the damping and stiffness characteristics associated with the body index, respectively. $x$ is the depth of the probe compressing the body tissue, and $F_c$ is the contact force between the probe and the body. Impedance parameters vary substantially for different tissue types, e.g., $K_d$ in the thoracic or skull region is considerably greater than that in the abdomen. Therefore, in an area with a large $K_d$, a minor movement of the probe position can lead to a substantial change in the contact force. In addition, the signal fed back to the controller from the pressure sensor cannot be completely equal to the desired value $F_d$, owing to noise. Therefore, it is necessary to provide a threshold value $\mu$ to keep the probe position constant when the measured pressure value is within the range of $F_d \pm \mu$. The threshold value can effectively improve the quality of US imaging by eliminating
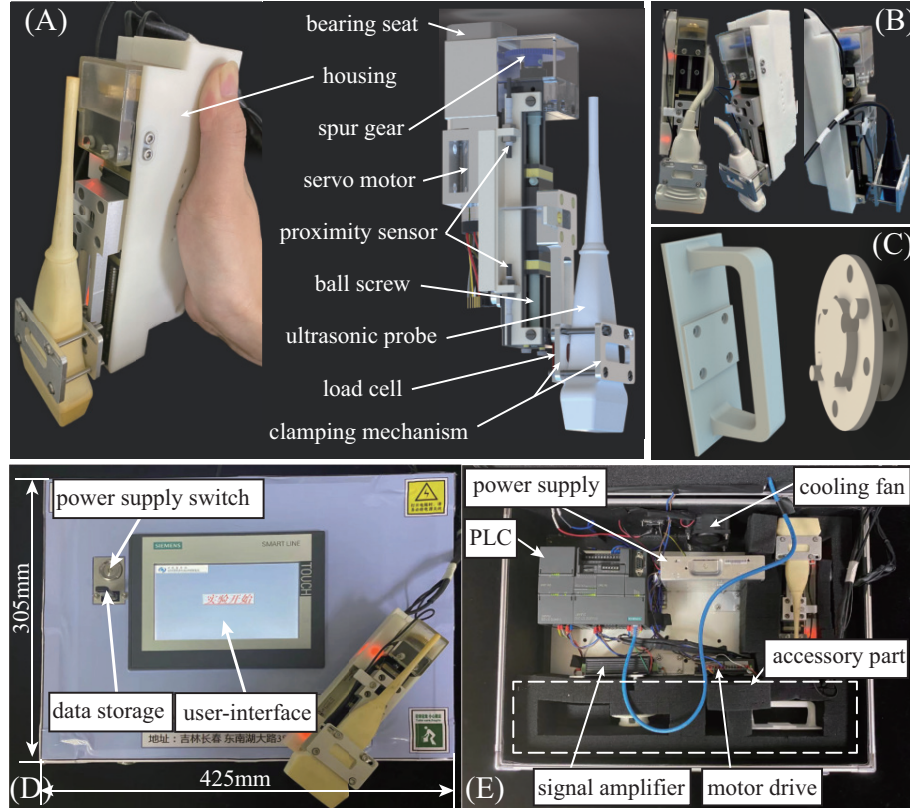
Fig. 1. Design of the PUAD mechanical system: (A) Physical drawing and model rendering of PUAD. (B) The PUAD mounted with different probes. (C) Designed handle for sonographers to hold the PUAD and the accessories to connect the manipulator. (D) External design of the control box. (E) Internal design of the control box.
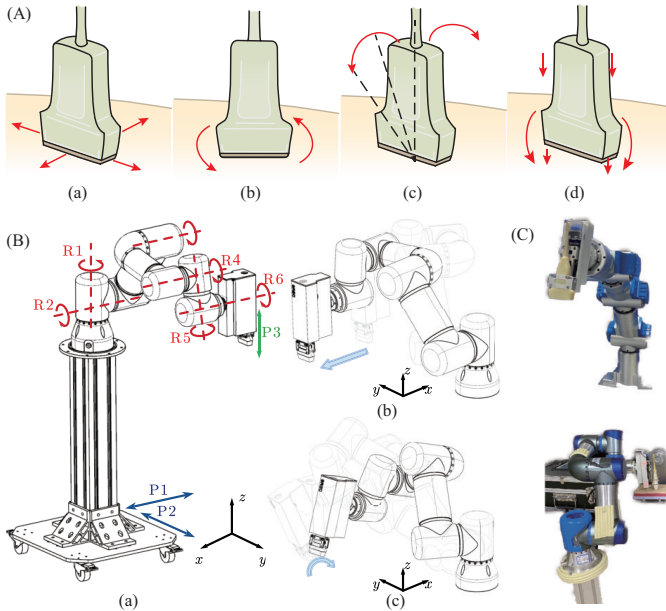


Fig. 2. The robotic manipulator system with the PUAD: (A) The four probe movements during US imaging, including (a) sliding, (b) rotation, (c) tilting, and (d) rocking. (B) Motion of the robotic manipulator integrated with the PUAD. (C) Different robotic manipulators installed with the PUAD, including a 7-DOF and 6-ODF manipulator.

chattering when detecting high-stiffness tissues, while also reducing energy consumption and improving the service life

of the motor.

A simple system–motion model was built for analysis to illustrate the effect of the defined threshold value on the control effect of the PUAD system. As shown in Fig. 3, we assume that the sonographer holds the end of the PUAD, whose position is defined as $x_0$. Because the sonographer's hand is prone to involuntary tremors over time, we assume $x_0(t) = 230 \, (t \leqslant 10 \text{ s})$, and $x_0(t) = 230 + 2\sin(20\pi t) \ (t > 10 \text{ s})$. Using the pressure error as the input signal to the PD controller, the speed of the motor can be expressed as:

$$r = k_p (F_d - F_c) + k_d \left( \dot{F}_d - \dot{F}_c \right), \tag{2}$$

where $k_p$ and $k_d$ are defined as control parameters. The moving speed of the probe can then be obtained as:

$$v = r * I * p + \dot{x}_0, \tag{3}$$

where $I = 1$ is the gear ratio, and $p = 2$ mm is the lead of the screw. The upper limit position of the slider at the screw is set as the initial position; it is then easy to obtain the position of the end of the probe as follows:

$$x_1 = x_0(t) - h_\perp - vt, \tag{4}$$

where $h_\perp = 200$ mm indicates the distance between the end of the probe and $x_0$ when the slider is in the upper limit position of the screw. According to the impedance relationship (1), the
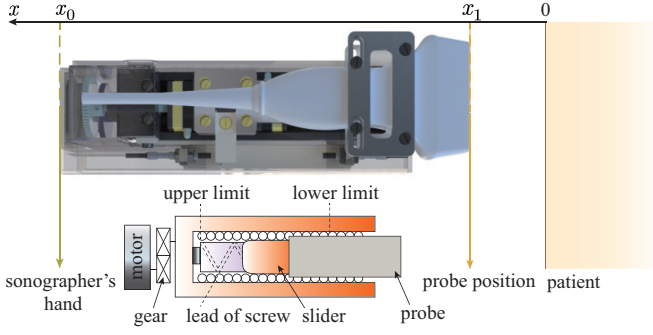
Fig. 3. Schematic of the PUAD system movement.

contact force between the probe and subject can be obtained as follows:

$$F_c = K_d \left( x_2 - x_1 \right) + B_d \left( \dot{x}_2 - \dot{x}_1 \right), \quad (5)$$

where $x_2$ denotes the position of the subject. For convenience of calculation, it is assumed that the position remains constant, and $x_2 = 0$.

According to [42], [43], the stiffness values range from 40 N/m to 44000 N/m and the damping values from 3.6 Ns/m to 175 Ns/m, with the large differences in stiffness between skeletal and soft tissues. Considering the silicone tissue used in our experiments, the impedance parameters were chosen as $K_d = 800$ N/m and $B_d = 10$ Ns/m, respectively. Based on empirical and trial-and-error methods, the parameters of the PD controller can be set as $k_p = 2$ and $k_d = 0.1$ for most US examinations, thus the parameters of the PD controller are not required to be retuned in operation. The maximum speed of the motor was set to 10 rev/s, and the lower limit position $h_\top$ of the slider was assumed to be 252 mm. To reflect the influence of pressure-sensor noise on the system, we provided a feedback pressure signal, which was a band-limited white noise with a noise power of 0.01, as shown in Fig. 4. It can be observed that even when the position $x_0$ is constant, the motor drives the probe in a reciprocating motion under the influence of noise if there is no defined threshold. When the threshold value is small, the continuous reciprocating rotation of the motor does not reduce. A large value results in a large tracking pressure error. Therefore, different pressure thresholds should be reasonably set when performing US scans of different parts of the body.

### B. Combined force and position control

The designed PUAD adopts a closed-loop force and position control strategy. As shown in Fig. 5, this control system can be switched to position-control mode or force-control mode. In force-control mode, we can avoid the probe from returning to its limit position when there is no contact with the subject in the initial state by setting a small start-up value (0.5 N), that is, the motor is driven only when the device switches to force-control mode and is subjected to a contact force greater than 0.5 N. When the force error exceeds a given threshold value, the force error is used as an input signal to the PD controller, and the output voltage is converted to current by the signal
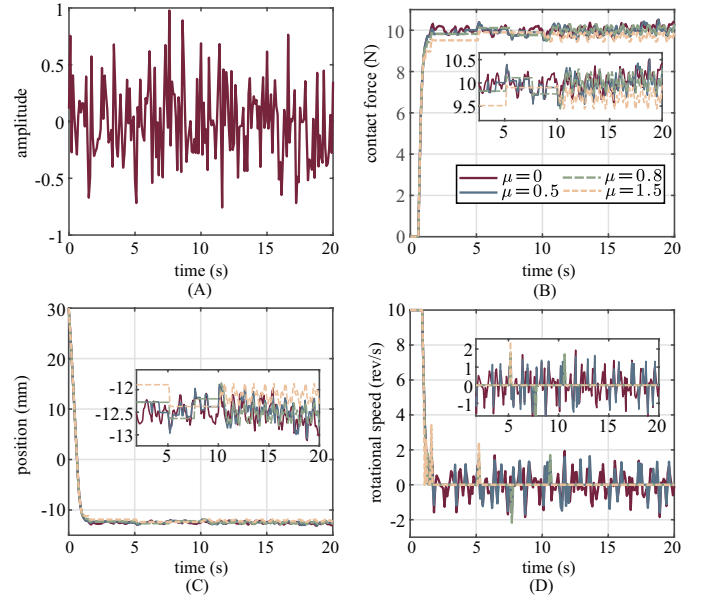


Fig. 4. Simulation results of the PUAD system for different pressure thresholds: (A) Noise applied by the pressure sensor during signal feedback. (B) Actual contact force at the end of the probe. (C) Position of the probe. (D) Rotation rate of the motor in the PUAD.
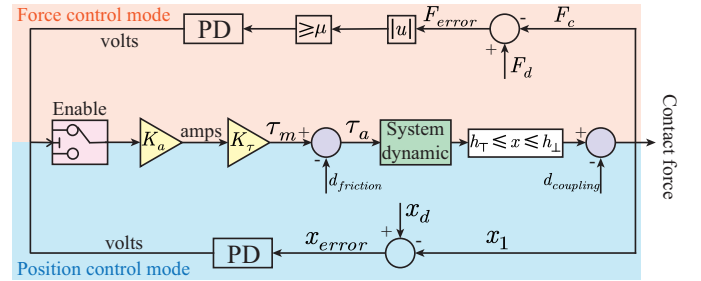


Fig. 5. Block diagram of closed-loop force and position control of the PUAD system.

amplifier $K_a$ and then passed to the motor. The motor converts the current to motor torque $\tau_m$ using the torque constant $K_\tau$. Considering the friction $d_{friction}$ in the motor movement, the actual torque $\tau_a$ is transmitted to the drive system. If the slider moves beyond the stroke limit, the photoelectric sensor triggers an interrupt signal to prevent the slider from continuing its movement. Notably, the position of the probe can be affected by external coupling disturbances $d_{coupling}$, including involuntary tremors of the sonographer's hand and changes in the subject's position. In the force control mode, the system exhibited an overdamped response with a steady-state error of 0.08 N (8%, $\mu = 0$) and a 10%-90% rise time of 0.08 s in a step response test of the target force from 4.0 to 5.0 N on a silicone tissue model.

## IV. EXPERIMENTS

In this section, a series of experiments were conducted to evaluate the performance of the designed device in US examinations, including the testing of device performance and three clinical application experiments.
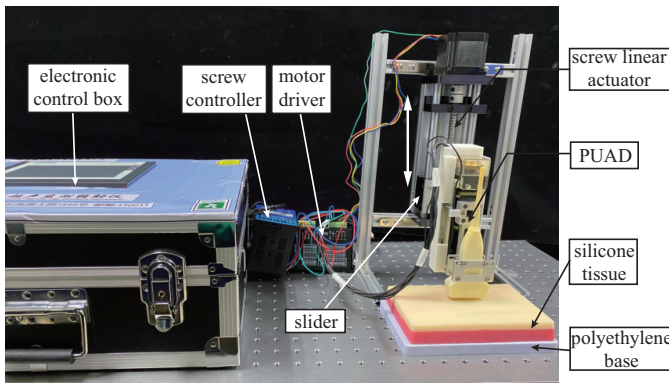
Fig. 6. Experimental setup for simulating the linear reciprocating motion of a human hand.
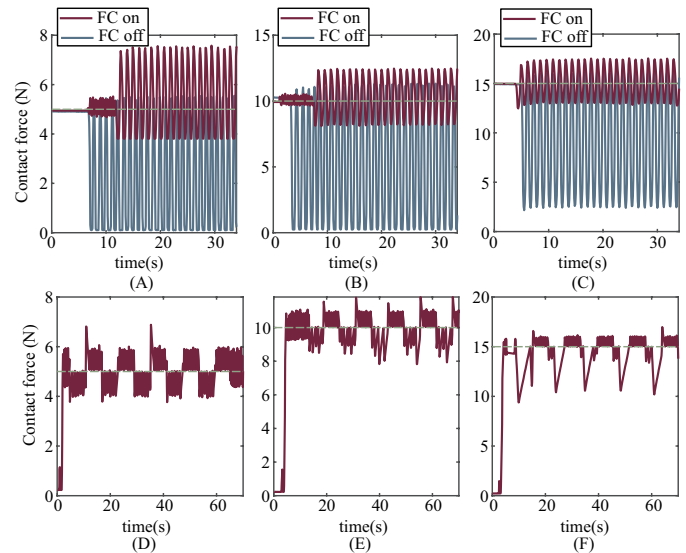


Fig. 7. Variation of contact force between probe and silicone tissue with time in simulated manual linear reciprocating-motion experiments: (A)–(C) Contact-force curves between the probe and silicone tissue over time for the PUAD with force-control mode on and off, under the condition that the slider moves at 4 cm/s, and the motion amplitude is 5 mm. The desired contact force is indicated by the green dashed line, and the actual contact force with the force control mode on and off is indicated by the red and blue lines, respectively. (D)–(F) Contact force curves between the probe and silicone tissue over time under the condition that the slider moves at a speed of 1 cm/s, and the motion amplitude is 4 cm.

## A. Experiments simulating sonographer tremor

During US examinations, the sonographer is prone to muscle soreness, owing to prolonged holding of the probe, which may lead to involuntary shaking. In this experiment, we simulated the contact force tracking of the PUAD system with different tremor amplitudes and frequencies. As shown in Fig. 6, the PUAD was vertically fixed on the slider of a screw driven by a stepper motor, and the stepper motor drove the slider to reciprocate and simulate a human hand. A silicone tissue was used to simulate the human muscle tissue, and a polyethylene base was used to represent the human bone.

To illustrate the contribution of the designed device to contact force compensation, pressure acquisition was performed with the PUAD system force-control mode turned on and off. In the first experiment, the movement speed of the screw linear actuator was set to 4 cm/s; the slide moved upward by 5 mm and then returned to its initial position and continued in a circular motion. The contact force between the probe and silicone tissue was first maintained at 5 N by adjusting the position of the screw slide. Then, the force-control mode of the PUAD was turned on, the tracking force contact was set to 5 N, and the force threshold was set to 0.8 N. We operated the screw slide in a reciprocating motion and recorded the contact force between the probe and silicone tissue. Next, the above experiment was repeated with force-control mode turned off to measure the changes in the contact force. Similarly, data on the contact forces were acquired using the PUAD to track the 10 N and 15 N forces.

As shown in Fig. 7, when force-control mode was turned off and the desired force was 5 N or 10 N, the end of the probe was completely detached from the silicone tissue with the upward movement of the slide. In contrast, when force-control mode was turned on, the contact force of the probe remained close to the desired contact force with a much smaller range of variation compared to that when force-control mode was off. In particular, the advantage of the PUAD was more apparent when the desired tracking pressure was higher, as shown in Fig. 7(C).

In the second experiment, we set the movement speed of the screw slide to 1 cm/s and the movement distance to 4 cm. The force-control mode of the PUAD was turned on to track

contact forces of 5 N, 10 N, and 15 N. As shown in Fig. 7, the device still achieves good force-tracking performance in force-control mode at a slow speed and large movement. Note that there is a substantial change in the contact force between the probe and silicone tissue at a tracking force of 15 N, as shown in Fig. 7(F), which is due to the large stiffness characteristics of the polyethylene base beneath the silicone tissue when the probe compresses the silicone tissue at a considerable depth. Therefore, a change in the position of the probe results to a substantial change in the contact force, which is consistent with the probe compressing rigid tissues (e.g., bone) in the body during US examinations.

## B. Experiments simulating subject movement

When performing a US examination, physiological behaviors, such as organ movement and breathing, inevitably lead to changes in the location of the tissues. It can be challenging for a sonographer to maintain consistent contact at all times, particularly for subjects undergoing prolong US examinations. In this experiment, a stepper motor was used to drive a precision lifting platform in a sinusoidal motion to simulate changes in the position of the subject, as shown in Fig. 8. We tested the tracking of the device for the desired contact force of 5 N at different force thresholds, and the experimental results are shown in Fig. 9. It was observed that the fluctuation of the contact force between the probe and silicone tissue was small with a small threshold, but the fluctuation frequency was high, which is consistent with the simulation results in Section III A. At different thresholds, the error between the contact force
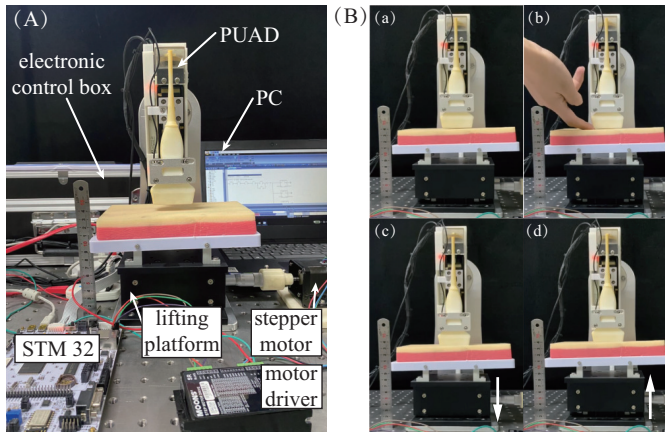
Fig. 8. Experiment simulating the subject's motion at a detection site: (A) Experimental setup. (B) Experimental procedure: (a) The PUAD was set to force-control mode, and the initial position of the probe was adjusted to ensure that the probe was not in contact with the silicone tissue. (b) A contact force was given to the end of the probe using a finger to start the PUAD movement and achieve the desired contact force. (c) The stepper motor drove the lift to slide downward in a sinusoidal curve. (d) The lift slide moved upward.
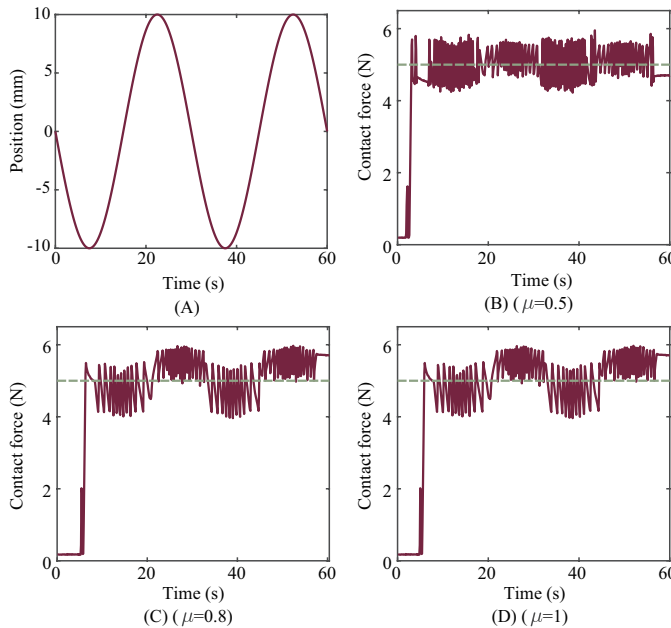


Fig. 9. Experimental results of the simulated motion of a subject's US examinations site: (A) Displacement curve of the precision lift slide. (B)–(D) The contact force between the probe and silicone tissue with time when the pressure threshold of the PUAD was set to 0.5 N, 0.8 N, and 1 N, respectively; the green dotted line represents the desired contact force.

and desired force, as the silicone tissue moved, was no more than 1 N.

### C. PUAD user studies in force control assessment

In this experiment, we performed user studies to assess the performance of sonographers in prolonged US examinations using the PUAD. The experience of sonographers is considered to be a key factor in improving diagnostic ability; therefore, eight operators with different experience levels participated in this experiment, including four experienced sonographers (working for more than five years) and four volunteers (no US
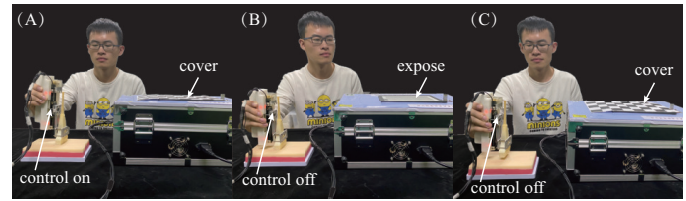


Fig. 10. The three scenarios in which the operator used the PUAD to maintain the desired contact force: (A) Automatic control. (B) Visual control. (C) Blind control.

related work experience). Experienced sonographers were employed in our experimental team, and inexperienced operators came from our team of volunteers with no clinical experience. The operators were asked to maintain a specified pressure of 5 N and 15 N for 3 min in each test. For a fair comparison, the operators were seated during each test, and a table supported their elbows. Each operator used the PUAD to maintain the desired pressure in the three scenarios shown in Fig. 10. The three scenarios are described as follows:

1) Automatic control: the force-control mode of the PUAD was switched on, the threshold was set to 0.5 N, and the operators were not allowed to observe the pressure value displayed on the control box.
2) Visual control: the force-control mode of the PUAD was turned off, but the operators were allowed to observe the displayed pressure values. The operators were required to autonomously adjust the contact force between the probe and silicone tissue.
3) Blind control: the force-control mode of the PUAD was turned off. After the operators observed the pressure value up to the desired pressure, they were no longer allowed to observe the pressure value.

As shown in Fig. 11, the automatic and visual control enabled a substantially more stable force control performance compared to blind control. Based on the blind-control results shown in Fig. 11, inexperienced operators are more likely to produce large excursions in contact force compared with experienced sonographers, owing to the weaker force control of inexperienced operators. In some medical centers or emergency situations, there may be a shortage of physicians who specialize in US examination. When operating in automatic control mode, operators with different experience levels can obtain similar pressure profiles, which helps to reduce the experience required for sonographers. Moreover, the auto-controlled device responds quickly to probe-position adjustments to ensure the desired contact force when the pressure exceeds the set threshold. In contrast, operators typically need to spend more time adjusting the probe position in visual control mode, such as in (d-5). Although the chattering of the contact force was smaller in visual control mode in several tests, as in (e-15), sonographers cannot focus their attention on the detected pressure during actual US examinations because they need focus on the diagnosis of a subject's condition.

The operators performed the test again, and the only difference was that their elbow joints were unsupported to analyze and compare the effect of supported (S) and unsupported (NS)
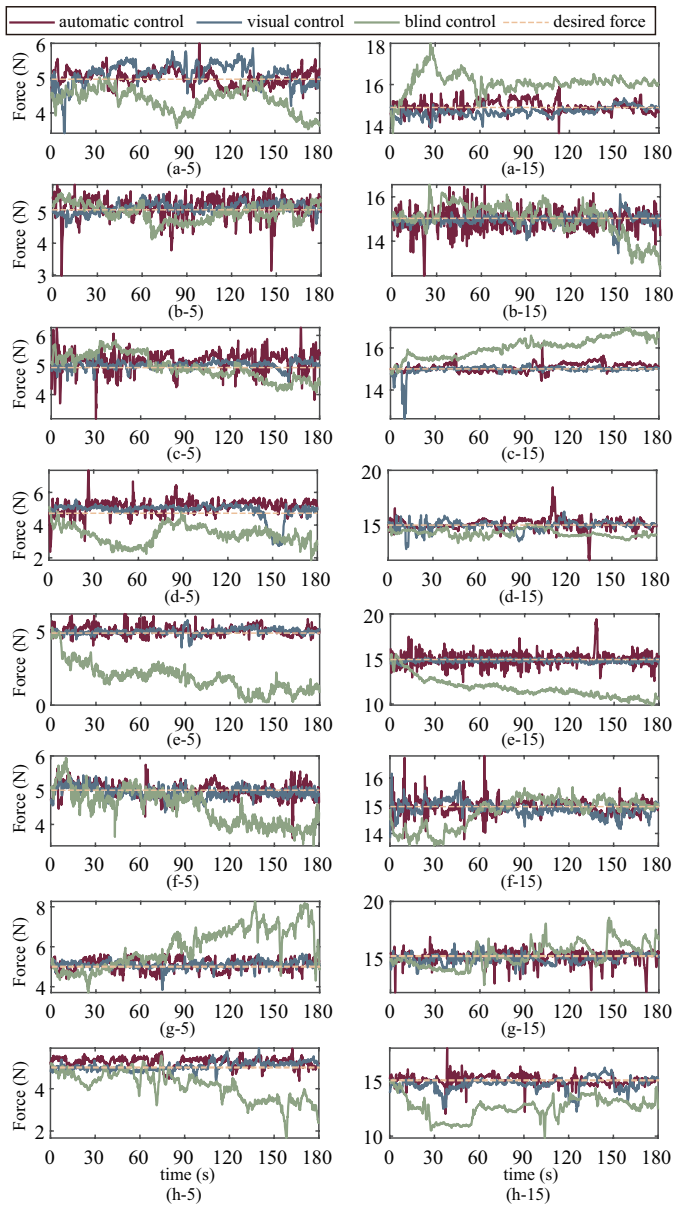
This article has been accepted for publication in IEEE Transactions on Ultrasonics, Ferroelectrics, and Frequency Control. This is the author's version which has not been fully edited and content may change prior to final publication. Citation information: DOI 10.1109/TUFFC.2022.3181287

8



Fig. 11. Contact forces obtained by eight operators in the three scenarios versus time: (a)–(h) indicate eight different operators, where "a–d" are experienced sonographers, and "e–h" are inexperienced operators. The values "5" and "15" represent the desired contact force.
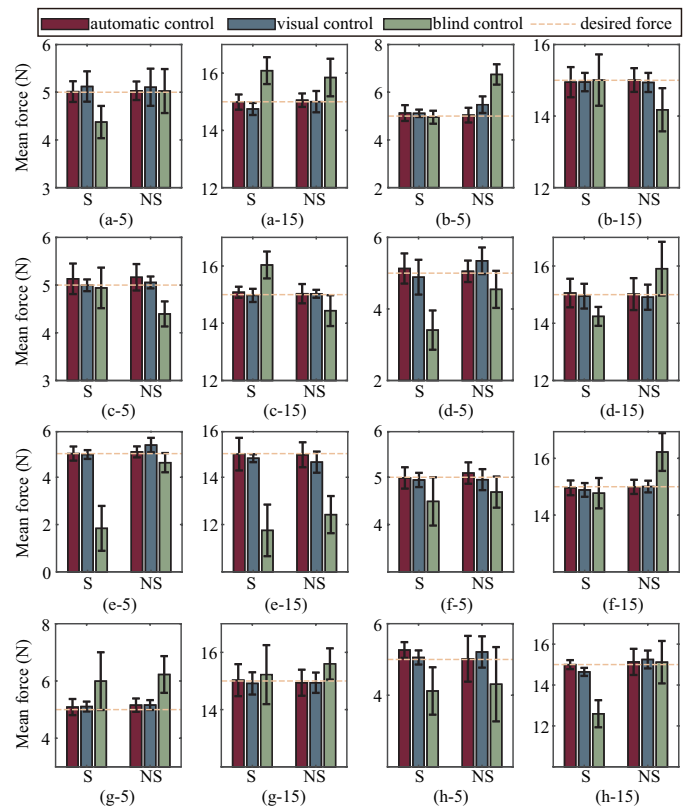


Fig. 12. Mean contact force and standard deviation for the eight operators in the three scenarios. Error bars are denoted as one standard deviation. (a)–(h) indicate eight different operators, where "a–d" are experienced sonographers, and "e–h" are inexperienced operators. The values "5" and "15" represent the desired contact force.

desired contact force after a period of testing, thereby resulting in changes in the contact force when adjusting the probe position. Although good control performance can be obtained with both automatic and visual control modes, sonographers are often unable to focus on observing pressure values or even obtaining them due to the requirement for timely patient diagnosis.

Further, a statistical analyses was performed in the R computing environment (version 4.1.2, R Core Team, 2019) to illustrate the statistical significance of the proposed test results. We used permutational multivariate ANOVA (PERMANOVA) with the "adonis" function to test the difference of the experimental data under the three factors (Pressure value 5N/15N, Supported/Unsupported, Experienced/Inexperienced), and the results were shown in Fig. 13.

The analysis showed that the three scenarios of automatic control, visual control, and blind control were all significantly different at the desired pressure conditions of 5 N and 15 N due to different desired pressures ($P < 0.001$). In the 5 N condition of the visual control mode, there was a significant difference between the NS and S groups ($P < 0.05$). For the 15 N condition in the blind control mode, the experimental results were significantly different ($P < 0.05$), and the data for experienced operators in the S group were significantly closer to the desired value compared to inexperienced operators, indicating that experienced operators have better force perception. In the

elbow joints on the contact force. As shown in Fig. 12, in the automatic control mode, the average contact force of the eight operators was almost the same as the desired contact force, and it was independent of experience and whether or not the elbow joint was supported. There is a small error between the average contact force and the desired contact force in the visual control mode, but the standard error is generally smaller than that of the automatic control. This may be because the operators can still hold the probe stably in three minutes while observing the displayed pressure. In the blind control mode, the average contact force differs substantially from the desired value, particularly for the inexperienced operators. In addition, operators produce large standard errors in the blind control mode, owing to the operators' decreased perception of the
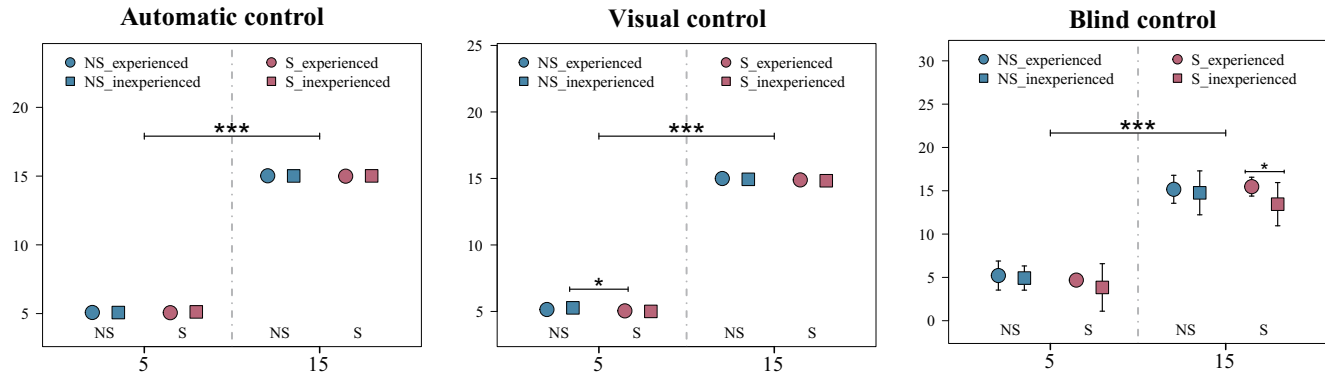
Fig. 13. Differences in automatic control, visual control and blind control among the desired pressure values in supported and unsupported elbow joints samples. NS = unsupported elbow joints, S= supported elbow joints. The error bars represent standard error. *: P < 0.05, **: P < 0.01, ***: P < 0.001.

automatic control mode, experience differences do not lead to significant differences in the results, then we can infer that by using the designed device, the differences in force perception ability between operators with different experience can be reduced. Meanwhile, it can be seen that the mean values of the contact forces in the automatic and visual control scenarios are closer to the desired values and have significantly smaller standard error; therefore, they have better control performance compared to the blind control scenario, which is consistent with our previous discussion.

### D. Conformity assessment of cervical vascular US images by PUAD

It is difficult to maintain consistency between two detection pressures at different times for US examinations. Moreover, different pressures result in different US images, which poses a diagnostic challenge for sonographers. Because the human neck has many blood vessels that are primarily superficial, sonographers need to compress the US probe on the skin using small contact force. Variations in contact force during examinations leads to substantial differences in US diagnostic results.

In this experiment, we compared the examination results obtained using the force-control mode of the PUAD and the traditional freehand US to assess the consistency of the diagnostic results. This subject is an adult male, 27 years of age, in good health. US examinations in this paper were performed using the Doppler US system (HI VISION Ascendus, Hitachi Aloka Medical Ltd., Tokyo, Japan) with a 5-13 MHz linear array transducer. Cervical vascular evaluations were performed according to the protocol we published earlier [44]. As shown in Fig. 14, three experienced sonographers (working for more than five years) performed US examinations on two segments of bilateral internal jugular vein (LJ2, LJ3, RJ2, and RJ3), and bilateral vertebral vein (LVV, RVV) of the same subject, respectively. Each sonographer first performed a freehand examination of the six vessels of the subject. They then repeated the examination using the force-control mode of the PUAD and recorded the detected cross-sectional area (CSA) and time-average-mean velocity (TAMV) of the vessels. The following day, the sonographers followed the same procedure

as the previous day, and the error of the experimental data for both days is shown in Fig. 15. The error of the two freehand US examination results was not substantially different from that of the PUAD, owing to the thin vascular LVV and RVV vessels. However, for other vessels, the concordance of almost all detections using PUAD was substantially better than that of the freehand US examination. The mean errors of the CSA obtained by the three sonographers using a freehand measurement and the PUAD were 0.098 and 0.048, respectively, with a 51% improvement in agreement. The TAMV errors were 9.428 and 4.072, respectively, with a 56.8% improvement in agreement. Experimental results show that the PUAD can effectively improve the consistency of diagnostic results when sonographers perform US examinations, which reduces the risk of physician misdiagnosis.

### E. Ultrasound assessment of leg muscles by PUAD

In contrast to the neck vessels, US scanning of the leg muscles requires compression of the vessels to a closed state with high pressure to facilitate US imaging of the muscles.

In this experiment, we asked three experienced sonographers (working for more than five years) to perform the US scan along the leg of a subject with force-control mode of the PUAD turned on and off, and we measured the contact force of the probe and obtained US images during the scan. Inexperienced volunteers were not employed in this experiment considering safety, operational difficulty, and the fact that we have demonstrated better force control by experienced sonographers in Section IV C. This subject was the same as in Section IV D, and lower extremity vascular evaluations were performed according to previous protocol [45]. All venous segments were examined in real-time B-mode using color Doppler in transverse and longitudinal views. As can be observed in Fig. 16, none of the vessels were completely compressed to a closed state when the force-control mode of the PUAD was turned off to perform the US scan. The sonographer focused on the US image instead of the probe in their hands; thus, the contact force on the probe was unconsciously reduced over time. It is also evident that even for the same areas, the contact force applied during the scan varied considerably from one sonographer to another. When

This article has been accepted for publication in IEEE Transactions on Ultrasonics, Ferroelectrics, and Frequency Control. This is the author's version which has not been fully edited and content may change prior to final publication. Citation information: DOI 10.1109/TUFFC.2022.3181287

10



Fig. 14. A sonographer using the PUAD to perform US examinations on the neck vessels of the subject.



Fig. 16. Result of the sonographers performing US scans on a leg with the force-control mode turned on and off. (A)–(C) denotes the three sonographers, "a" denotes force-control mode switched off, "b" denotes force-control mode switched on, and the blood vessels of the leg are in the yellow box.
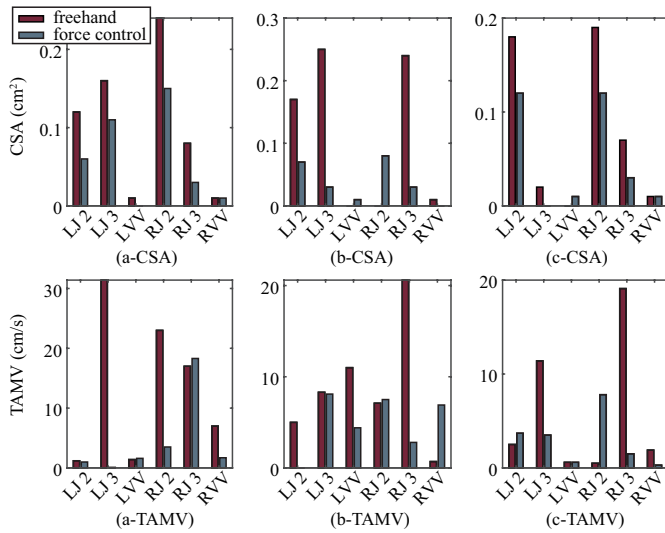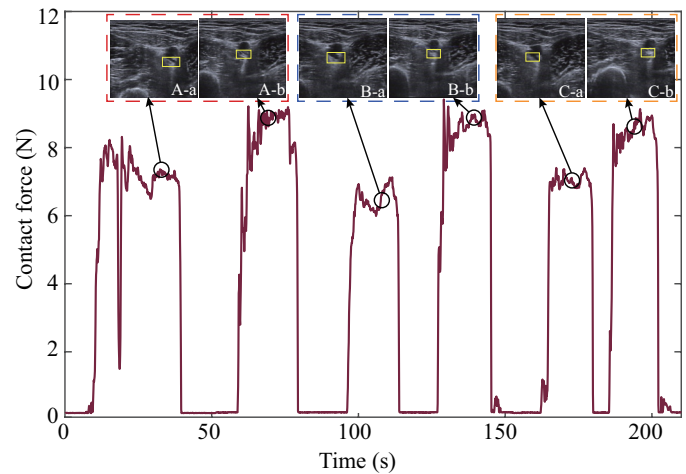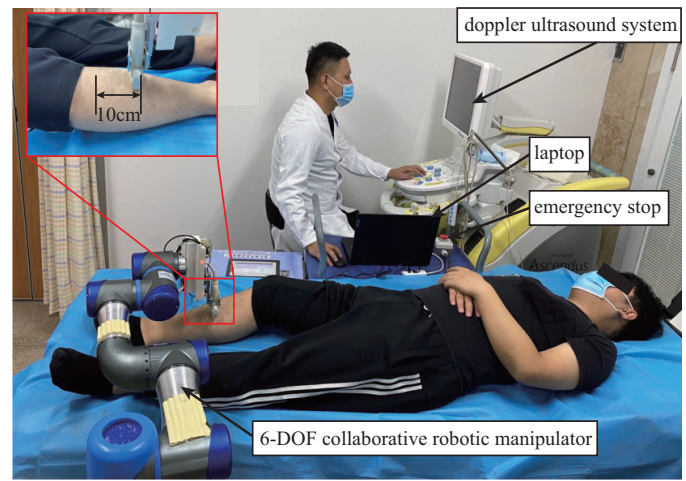


Fig. 15. Errors of the data from two tests using force-control mode of the PUAD and freehand US examinations. (a)–(c) denotes each of three sonographers, respectively.



Fig. 17. A sonographer performing US scans of a subject's leg using a robotic manipulator with a PUAD.

the US scan of the leg was performed in the force-control mode, the contact force was substantially greater than when it was turned off, and all blood vessels in the leg were pressed to closure. As a result, the sonographers could focus more on diagnosing conditions rather than on the contact force of the probe when using the PUAD for US examinations.

### F. Ultrasound experiments with a manipulator integrated with PUAD

As described in Section II-C, the PUAD can be fixed to the end of a robot manipulator as a robotic US system. To illustrate the performance of a manipulator integrated with the PUAD, we performed a scanning experiment on the leg of a subject using a robotic US system. As shown in Fig. 17, the PUAD was mounted on a 6-DOF collaborative robotic manipulator, and US scans were performed on the calf muscles, within a 10 cm wide plane, of 14 subjects, respectively. These subjects were employed in our experimental team and included men

and women of various ages. The robotic system did not have a force-sensing capability; therefore, it was only used to perform reciprocating linear movements within the plane. The PUAD regulated the contact force between the probe and the subject, and the desired pressure value was set to 6 N. To demonstrate the threshold effect on the contact force, we set the following thresholds for the device to be sonicated: 0.8 N, 0.6 N, 0.4 N, and 0.1 N.

The experimental results are shown in Fig. 18, and it can be seen that the designed device is able to achieve effective tracking of the desired pressure for different subjects. It is worth mentioning that for subjects of different ages, genders and physical conditions, their calf muscles can vary considerably. Several spikes of contact force can be seen in Fig. 18 (K) and (L), which is due to the gastrocnemius muscle is stronger in both subjects and therefore there is a large abrupt change in contact force when the probe is swept through. Even in Fig. 18 (L), there is a brief detachment of the probe from the leg of the subject, which causes the contact force to become zero. With

This article has been accepted for publication in IEEE Transactions on Ultrasonics, Ferroelectrics, and Frequency Control. This is the author's version which has not been fully edited and content may change prior to final publication. Citation information: DOI 10.1109/TUFFC.2022.3181287
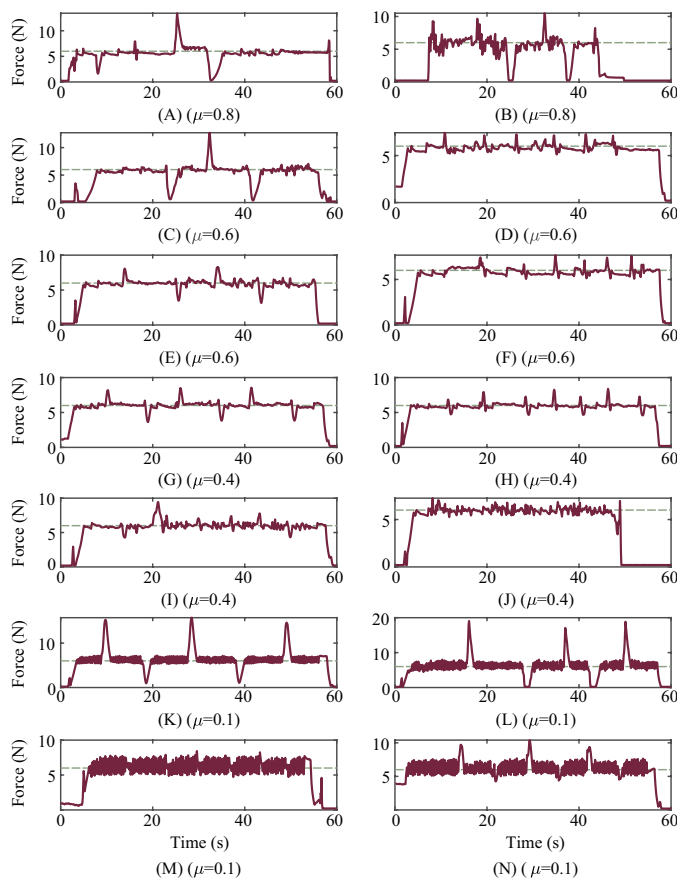
11



Fig. 18. Pressure curves obtained via the US scanning of the legs of each subject using the robotic US system. (A)–(N) represents each subject. The green dotted lines indicate the desired pressure value.

the rapid response of the PUAD, the contact force of the probe can quickly reach the desired pressure. Especially, a smooth contact force was always maintained during the US scanning when the pressure thresholds were set to 0.4 N and 0.6 N. For example, in Fig. 18 (J), the error between the contact force of the probe and the desired value is always less than 1 N. This indicates that the robotic US system can perform some simple tasks, which can effectively reduce the work intensity of the sonographer.

## V. DISCUSSION AND FUTURE WORK

### A. Advantages and Applications

This paper describes a miniaturized device (PUAD) for assisted sonography and its mechanical design, control, modeling, and several device evaluations. The experimental results obtained demonstrate three substantial advantages of utilizing the PUAD in US scanning. First, by introducing force thresholds in the controller, the difficulty in applying existing automatic control devices, highlighted in [35]–[39], to challenging tissue imaging of the human body was effectively solved. Therefore, the designed device can assist sonographers in maintaining a stable contact force between the probe and a subject, regardless of the movement of the sonographer's hand or the subject. This is particularly important for inexperienced sonographers. The PUAD can improve their ability to apply

the appropriate level of force, and visualizing pressure values is beneficial for them to quickly master the US examination technique. Moreover, the consistency of the US results was substantially improved by applying force control. That is, the designed device enables a simple method to compare US images acquired at different times, which provides the sonographer with an additional diagnostic tool to assess changes in the characteristics of tissues over time. Finally, the device effectively helps sonographers maintain the suitable contact force, which improves imaging quality during US examinations.

In the experiment with the robotic manipulator, the sonographers were only required to operate the robotic manipulator to the position to be tested, and the PUAD automatically controlled the contact force. The operational difficulty experienced by a sonographer when using this device was considerably reduced compared with devices that require both position and pressure control by operators [17]. Owing to the widespread applications of US imaging technology, the designed PUAD can improve existing diagnostic US techniques and contribute to the improvement of the diagnostic capabilities of primary sonographers. Although the health benefits of the PUAD to sonographers are not discussed in this paper, the device changes the traditional way that a sonographer holds the probe, which may help alleviate the high prevalence of musculoskeletal symptoms among sonographers.

Besides the direct improvement of US imaging quality, estimation of tissue elasticity by applying a brief mechanical excitation to the tissue surface can be very useful in clinical medicine. Although this was not the focus of our current study, the results of related studies [1], [25] and the experimental results in this paper suggest that the designed device also has great potential for application in elastography.

### B. Limitations

Although the designed device can automatically track the desired pressure, compared to some freehand devices used only for the acquisition of probe pressure [30], [31], the size and mass of the device makes it more suitable for US examinations of the legs, abdomen, and other areas that are not easily restricted. Moreover, operators can adjust the pressure threshold to make the device respond to tissues of different stiffness levels, but this is dependent on their clinical experience. The adaptive control technique may be an effective way to assist operators in setting reasonable pressure thresholds, i.e., the device obtains the impedance parameters of the region to be detected by fast active motion and then determines the appropriate threshold. Despite the potential benefits that medical robotics can bring to US diagnostics, the development of robotics in the field of US remains a relatively slow process compared with the rapid development of industrial robotics, owing to the complexity of the operating procedures and the strict requirements for safety.

### C. Security

Ensuring the safety of medical devices is an important issue, but many existing designs ignore the analysis of safety

[33]–[35]. For the designed PUAD, we have considered the following measures to guarantee its security. Firstly, to prevent the probe from exerting too much force on the subject, the probe can automatically return to its original position when the detected pressure exceeds 25 N, and the power supply of the designed device is ready to be disconnected by the operator once it suffers component failure. Additionally, one of the most important advantages of the PLC as the controller of the PUAD is its high reliability and anti-interference, with almost no risk of burnout during start-up and operation. The control box is equipped with a fan for heat dissipation and some sponges for cushioning to improve the safety of the device during operation. Finally, the control box is a sturdy aluminum alloy air box and is closed during operation, which can also ensure the safety of the operator.

### D. Future work

The programmable controller in PUAD makes it highly extensible, so more functions can be developed on demand than only mentioned in this paper. Future work will focus on the design of controllers that allow the adaptive adjustment of device thresholds to improve efficiency and reduce operational difficulties. Moreover, remote US diagnosis via autonomous robotic US acquisition is a meaningful research direction [43]; it improves accessibility to a high standard of care and ensures the safety of the sonographer. By combining the robotic manipulator with the PUAD, we reduced the difficulty of force control when using a robotic US system. However, there are still some system limitations, such as possible communication delays and inaccurate inspection positions in remote operations. We expect that future US diagnostic devices will aim towards artificial intelligence and decision making by learning from the clinical experience of physicians. As this is beyond the scope of the current study, we will conduct further research in this field in potential future work.

## VI. CONCLUSION

In this study, we proposed a device to assist sonographers with contact-force control that supports accurate and straightforward diagnosis. We established a control system using integrated hardware and software, and the device was integrated in a conventional ultrasound (US) equipment to compensate for physiological motion. By setting the pressure threshold, the device was applied to US examinations of tissues of different degrees of hardness in the human body. The experimental results show that the designed device helps to reduce the requirements for the clinical experience of sonographers, and it improves the consistency of detection results and the quality of US images. Moreover, the designed device can be flexibly combined with different robotic manipulators, which has excellent potential for future remote or automated US examinations. Although the designed device has been experimentally validated for its superior performance, further improvements in miniaturization, control, and cost of manipulable technology are needed to increase its widespread use.

## REFERENCES

[1] R. Z. Azar, K. Dickie, and L. Pelissier, "Real-time 1-d/2-d transient elastography on a standard ultrasound scanner using mechanically induced vibration," *IEEE transactions on ultrasonics, ferroelectrics, and frequency control*, vol. 59, no. 10, pp. 2167–2177, 2012.

[2] K. K. Shung, "Diagnostic ultrasound: Past, present, and future," *J Med Biol Eng*, vol. 31, no. 6, pp. 371–4, 2011.

[3] N. Velez, D. E. Earnest, and E. D. Staren, "Diagnostic and interventional ultrasound for breast disease," *The American journal of surgery*, vol. 180, no. 4, pp. 284–287, 2000.

[4] A. Liebeskind, A. G. Sikora, A. Komisar, D. Slavit, and K. Fried, "Rates of malignancy in incidentally discovered thyroid nodules evaluated with sonography and fine-needle aspiration," *Journal of ultrasound in medicine*, vol. 24, no. 5, pp. 629–634, 2005.

[5] J. R. Roelandt, "Ultrasound stethoscopy: a renaissance of the physical examination?" 2003.

[6] K. Li, Y. Xu, and M. Q.-H. Meng, "An overview of systems and techniques for autonomous robotic ultrasound acquisitions," *IEEE Transactions on Medical Robotics and Bionics*, 2021.

[7] A. Kaminski, A. Payne, S. Roemer, D. Ignatowski, and B. K. Khandheria, "Answering to the call of critically ill patients: limiting sonographer exposure to covid-19 with focused protocols," *Journal of the American Society of Echocardiography*, vol. 33, no. 7, pp. 902–903, 2020.

[8] H. E. Vanderpool, E. A. Friis, B. S. Smith, and K. L. Harms, "Prevalence of carpal tunnel syndrome and other work-related musculoskeletal problems in cardiac sonographers." *Journal of occupational medicine.: official publication of the Industrial Medical Association*, vol. 35, no. 6, pp. 604–610, 1993.

[9] N. Magnavita, L. Bevilacqua, P. Mirk, A. Fileni, and N. Castellino, "Work-related musculoskeletal complaints in sonologists," *Journal of occupational and environmental medicine*, vol. 41, no. 11, pp. 981–988, 1999.

[10] C. Murphy and A. Russo, "An update on ergonomic issues in sonography," *Healthcare Benefit Trust*, 2000.

[11] M. B. Rominger, P. Kälin, M. Mastalerz, K. Martini, V. Klingmüller, S. Sanabria, and T. Frauenfelder, "Influencing factors of 2d shear wave elastography of the muscle–an ex vivo animal study," *Ultrasound international open*, vol. 4, no. 02, pp. E54–E60, 2018.

[12] T. A. Krouskop, T. M. Wheeler, F. Kallel, B. S. Garra, and T. Hall, "Elastic moduli of breast and prostate tissues under compression," *Ultrasonic imaging*, vol. 20, no. 4, pp. 260–274, 1998.

[13] S. Goswami, R. Ahmed, F. Feng, S. Khan, M. M. Doyley, and S. A. McAleavey, "Imaging the local nonlinear viscoelastic properties of soft tissues: Initial validation and expected benefits," *IEEE Transactions on Ultrasonics, Ferroelectrics, and Frequency Control*, 2022.

[14] A. Kuzmin, A. M. Zakrzewski, B. W. Anthony, and V. Lempitsky, "Multi-frame elastography using a handheld force-controlled ultrasound probe," *IEEE transactions on ultrasonics, ferroelectrics, and frequency control*, vol. 62, no. 8, pp. 1486–1500, 2015.

[15] M. R. Burcher, J. A. Noble, L. Man, and M. Gooding, "A system for simultaneously measuring contact force, ultrasound, and position information for use in force-based correction of freehand scanning," *ieee transactions on ultrasonics, ferroelectrics, and frequency control*, vol. 52, no. 8, pp. 1330–1342, 2005.

[16] D. I. Gendin, R. Nayak, Y. Wang, M. Bayat, R. T. Fazzio, A. A. Oberai, T. J. Hall, P. E. Barbone, A. Alizad, and M. Fatemi, "Repeatability of linear and nonlinear elastic modulus maps from repeat scans in the breast," *IEEE transactions on medical imaging*, vol. 40, no. 2, pp. 748–757, 2020.

[17] F. Pierrot, E. Dombre, E. Dégoulange, L. Urbain, P. Caron, S. Boudet, J. Gariépy, and J.-L. Mégnien, "Hippocrate: A safe robot arm for medical applications with force feedback," *Medical Image Analysis*, vol. 3, no. 3, pp. 285–300, 1999.

[18] Q. Huang, J. Lan, and X. Li, "Robotic arm based automatic ultrasound scanning for three-dimensional imaging," *IEEE Transactions on Industrial Informatics*, vol. 15, no. 2, pp. 1173–1182, 2018.

[19] Q. Huang, B. Wu, J. Lan, and X. Li, "Fully automatic three-dimensional ultrasound imaging based on conventional b-scan," *IEEE transactions on biomedical circuits and systems*, vol. 12, no. 2, pp. 426–436, 2018.

[20] M. K. Welleweerd, A. G. de Groot, S. de Looijer, F. J. Siepel, and S. Stramigioli, "Automated robotic breast ultrasound acquisition using ultrasound feedback," in *2020 IEEE International Conference on Robotics and Automation (ICRA)*, pp. 9946–9952. IEEE, 2020.

[21] Z. Jiang, M. Grimm, M. Zhou, Y. Hu, J. Esteban, and N. Navab, "Automatic force-based probe positioning for precise robotic ultrasound

acquisition," *IEEE Transactions on Industrial Electronics*, vol. 68, no. 11, pp. 11 200–11 211, 2020.

[22] Z. Jiang, Y. Zhou, Y. Bi, M. Zhou, T. Wendler, and N. Navab, "Deformation-aware robotic 3d ultrasound," *IEEE Robotics and Automation Letters*, vol. 6, no. 4, pp. 7675–7682, 2021.

[23] F. Suligoj, C. M. Heunis, J. Sikorski, and S. Misra, "Robust–an autonomous robotic ultrasound system for medical imaging," *IEEE Access*, vol. 9, pp. 67 456–67 465, 2021.

[24] W.-H. Zhu, S. E. Salcudean, S. Bachmann, and P. Abolmaesumi, "Motion/force/image control of a diagnostic ultrasound robot," in *Proceedings 2000 ICRA. Millennium Conference. IEEE International Conference on Robotics and Automation. Symposia Proceedings (Cat. No. 00CH37065)*, vol. 2, pp. 1580–1585. IEEE, 2000.

[25] P. Abolmaesumi, S. E. Salcudean, W.-H. Zhu, M. R. Sirouspour, and S. P. DiMaio, "Image-guided control of a robot for medical ultrasound," *IEEE Transactions on Robotics and Automation*, vol. 18, no. 1, pp. 11–23, 2002.

[26] S. E. Salcudean, G. Bell, S. Bachmann, W.-H. Zhu, P. Abolmaesumi, and P. D. Lawrence, "Robot-assisted diagnostic ultrasound–design and feasibility experiments," in *International Conference on Medical Image Computing and Computer-Assisted Intervention*, pp. 1062–1071. Springer, 1999.

[27] S. Lessard, P. Bigras, and I. A. Bonev, "A new medical parallel robot and its static balancing optimization," 2007.

[28] A. Vilchis, J. Troccaz, P. Cinquin, K. Masuda, and F. Pellissier, "A new robot architecture for tele-echography," *IEEE Transactions on Robotics and Automation*, vol. 19, no. 5, pp. 922–926, 2003.

[29] P. J. Berkelman, P. Cinquin, J. Troccaz, J.-M. Ayoubi, and C. Létoublon, "Development of a compact cable-driven laparoscopic endoscope manipulator," in *International Conference on Medical Image Computing and Computer-Assisted Intervention*, pp. 17–24. Springer, 2002.

[30] T. Schimmoeller, R. Colbrunn, T. Nagle, M. Lobosky, E. E. Neumann, T. M. Owings, B. Landis, J. E. Jelovsek, and A. Erdemir, "Instrumentation of off-the-shelf ultrasound system for measurement of probe forces during freehand imaging," *Journal of biomechanics*, vol. 83, pp. 117–124, 2019.

[31] M. W. Gilbertson and B. W. Anthony, "An ergonomic, instrumented ultrasound probe for 6-axis force/torque measurement," in *2013 35th Annual International Conference of the IEEE Engineering in Medicine and Biology Society (EMBC)*, pp. 140–143. IEEE, 2013.

[32] M. Dhyani, S. C. Roll, M. W. Gilbertson, M. Orlowski, A. Anvari, Q. Li, B. Anthony, and A. E. Samir, "A pilot study to precisely quantify forces applied by sonographers while scanning: A step toward reducing ergonomic injury," *Work*, vol. 58, no. 2, pp. 241–247, 2017.

[33] F. Eura, R. Aizawa, R. Kondo, K. Tomita, Y. Nishiyama, and N. Koizumi, "Development of portable ultrasound guided physiological motion compensation device," in *2017 IEEE International Conference on Cyborg and Bionic Systems (CBS)*, pp. 243–247. IEEE, 2017.

[34] M. Marchal and J. Troccaz, "A one-dof freehand haptic device for robotic tele-echography," *Studies in health technology and informatics*, pp. 231–233, 2004.

[35] M. W. Gilbertson and B. W. Anthony, "Impedance-controlled ultrasound probe," in *Medical Imaging 2011: Ultrasonic Imaging, Tomography, and Therapy*, vol. 7968, p. 796816. International Society for Optics and Photonics, 2011.

[36] M. W. Gilbertson and B. W. Anthony, "Ergonomic control strategies for a handheld force-controlled ultrasound probe," in *2012 IEEE/RSJ International Conference on Intelligent Robots and Systems*, pp. 1284–1291. IEEE, 2012.

[37] M. W. Gilbertson and B. W. Anthony, "Force and position control system for freehand ultrasound," *IEEE Transactions on Robotics*, vol. 31, no. 4, pp. 835–849, 2015.

[38] S. Koppaka, M. W. Gilbertson, S. B. Rutkove, and B. W. Anthony, "Evaluating the clinical relevance of force-correlated ultrasound," in *2014 IEEE 11th International Symposium on Biomedical Imaging (ISBI)*, pp. 1172–1175. IEEE, 2014.

[39] S. Koppaka, M. W. Gilbertson, J. S. Wu, S. B. Rutkove, and B. W. Anthony, "Assessing duchenne muscular dystrophy with force-controlled ultrasound," in *2014 IEEE 11th International Symposium on Biomedical Imaging (ISBI)*, pp. 694–697. IEEE, 2014.

[40] L. Birglen, C. Gosselin, N. Pouliot, B. Monsarrat, and T. Laliberté, "Shade, a new 3-dof haptic device," *IEEE Transactions on Robotics and Automation*, vol. 18, no. 2, pp. 166–175, 2002.

[41] H.-Y. Li, I. Paranawithana, L. Yang, T. S. K. Lim, S. Foong, F. C. Ng, and U.-X. Tan, "Stable and compliant motion of physical human–robot interaction coupled with a moving environment using variable ad-

mittance and adaptive control," *IEEE Robotics and Automation Letters*, vol. 3, no. 3, pp. 2493–2500, 2018.

[42] L. Wood, C. Suggs, and C. Abrams Jr, "Hand-arm vibration part iii: A distributed parameter dynamic model of the human hand-arm system," *Journal of Sound and Vibration*, vol. 57, no. 2, pp. 157–169, 1978.

[43] J. E. Speich, L. Shao, and M. Goldfarb, "Modeling the human hand as it interacts with a telemanipulation system," *Mechatronics*, vol. 15, no. 9, pp. 1127–1142, 2005.

[44] L. Liu, Y. Xing, Y. Chen, X. Ji, J. Ge, and L. Wang, "Eye-neck integrated ultrasound in idiopathic intracranial hypertension and cerebral venous sinus thrombosis," *Frontiers in Neurology*, vol. 12, 2021.

[45] L. Needleman, J. J. Cronan, M. P. Lilly, G. J. Merli, S. Adhikari, B. S. Hertzberg, M. R. DeJong, M. B. Streiff, and M. H. Meissner, "Ultrasound for lower extremity deep venous thrombosis: multidisciplinary recommendations from the society of radiologists in ultrasound consensus conference," *Circulation*, vol. 137, no. 14, pp. 1505–1515, 2018.